Progress In Electromagnetics Research M, Vol. 133, 51–60, 2025

PIER M

(Received 8 February 2025, Accepted 11 April 2025, Scheduled 23 April 2025)

Genetic Algorithm Optimization of a Wideband Rectangular Patch Antenna with an Asymmetric U-Slot and Partial Ground for Ku-Band Satellite Communication

Fatim-Zahra Benniouι[1], Asma Khabba[1,2], Karima Ait Bouslam[1], Layla Wakrim[3], Saida Ibnyaich[1], Abdelouhab Zeroual[1], Zahriladha Zakaria[4], and Ahmed J. A. Al-Gburi[4,*]

[1]*Instrumentation, Signals and Physical Systems (I2SP) Team, Faculty of Sciences Semlalia Cadi Ayyad University, Marrakesh, Morocco*
[2]*LAMIGEP Laboratory, Moroccan School of Engineering Sciences (EMSI), Marrakesh, Morocco*
[3]*Laboratory of Innovation in Management and Engineering for Business (LIMIE) Higher Institute of Engineering and Business (ISGA), Marrakesh, Morocco*
[4]*Center for Telecommunication Research & Innovation (CeTRI), Fakulti Teknologi Dan Kejuruteraan Elektronik Dan Komputer (FTKEK), Universiti Teknikal Malaysia Melaka (UTeM), Jalan Hang Tuah Jaya, Durian Tunggal, Melaka 76100, Malaysia*

ABSTRACT: This paper presents an innovative microstrip patch antenna (MPA) designed and optimized for Ku-band satellite communications. The proposed design incorporates an asymmetric U-shaped slot and a partial ground plane, constructed using an FR4 substrate with dimensions of $18 \times 16 \times 1.6\,\text{mm}^3$ ($0.416\lambda \times 0.37\lambda \times 0.03\lambda$, where λ is the wavelength at 6.94 GHz). A genetic algorithm is employed to optimize the U-shaped slot and ground plane dimensions, enhancing the antenna's wideband performance while preserving its compact form factor. Simulation results indicate that the optimized design achieves two operational frequency bands with reflection coefficients (S_{11}) less than -10 dB: a narrowband from 6.83 GHz to 7 GHz, with a resonant frequency of 6.94 GHz, and a wideband from 10.26 GHz to 17.19 GHz, with a resonant frequency of 14.94 GHz. This extensive frequency range enables the antenna to effectively support direct broadcast services (DBSs) and fixed satellite services (FSS). The design's effectiveness was confirmed through prototype fabrication and testing, demonstrating strong agreement with simulated results and proving the antenna's compactness and exceptional wideband performance.

1. INTRODUCTION

Satellite communications are vital for connecting our planet with space, enabling long-distance and remote communication in areas where traditional networks are impractical or prohibitively expensive. This advanced technology is utilized for various applications such as global broadcasting, multicasting, weather forecasting, navigation, emergency communications, and facilitating communication for space and interplanetary missions [1, 2]. As global connectivity expands, and the need for real-time data grows, the importance of satellite communications continues to increase.

Antennas are key components in satellite communication systems that transmit and receive signals over vast distances. As satellite technology evolves, there is a growing emphasis on designing compact antennas that integrate seamlessly into satellites while delivering high performance.

Microstrip Patch Antennas (MPAs) are highly favored for satellite communication due to their numerous benefits, such as simple geometry, lightweight construction, compact design, low profile, and cost efficiency. They are also straightforward to manufacture and can be adapted for planar and non-planar surfaces. However, MPAs are often limited by their narrow bandwidth [3].

To address these limitations, researchers have investigated several techniques to enhance the bandwidth of MPAs. These techniques include incorporating parasitic elements [4, 5], utilizing metamaterials [6], modifying the radiating plane geometry [7, 8], and modifying the ground plane [9, 10].

In response to the evolving demands of satellite communication applications, substantial research and development efforts are dedicated to developing innovative antenna solutions. Various designs have been proposed to fulfill the specific needs of Ku-band satellite systems, focusing on performance optimization and reliability enhancement. For instance, in [11], a wideband antenna for satellite applications, operating between 12.8 and 15.8 GHz, was presented. This design incorporates etched slots on the radiating element and a defective ground structure (DGS) to achieve its broad bandwidth. However, the antenna has a relatively large size of $40 \times 48 \times 1.59\,\text{mm}^3$. Similarly, [12] introduced a compact H-shaped patch antenna for Ku-band applications, offering a broad bandwidth of 4.1553 GHz, spanning from 11.595 GHz to 15.75 GHz. This design employs an etched I-slot on the radiating element to achieve its wideband characteristics. Despite its compact design, the antenna's overall size is $40 \times 40 \times 1.6\,\text{mm}^3$, which is still relatively large. The antenna

* Corresponding author: Ahmed Jamal Abdullah Al-Gburi (ahmedjamal@ieee.org/engahmed_jamall@yahoo.com).

doi:10.2528/PIERM25020802

discussed in [13] utilizes parasitic components in the shape of a double L. This design operates across a frequency range from 11.81 GHz to 18.47 GHz, providing a 6.66 GHz bandwidth. The double L-shaped parasitic elements enhance the antenna's bandwidth, but the overall size is $30 \times 30 \times 1.6\,\text{mm}^3$, which is considered large. In [14], a compact, dual circularly polarized antenna for the Ku band is designed, covering bandwidths from 12.3 GHz to 13.2 GHz and from 15.3 GHz to 16.3 GHz. Its size is $26 \times 27 \times 1.6\,\text{mm}^3$, which is also relatively large. Finally, [15] describes an MPA for Ku-band frequencies, offering a 2 GHz frequency range from 11 GHz to 13 GHz. The design includes a cap-shaped cut to improve impedance bandwidth. However, the antenna's dimensions are $20 \times 20 \times 1.6\,\text{mm}^3$, which, although compact, is still considered relatively large.

To address the challenge of designing a voluminous antenna, this paper presents a new method for creating a low-profile, miniature, wideband MPA. Our approach employs a genetic algorithm (GA) to fine-tune the size of the ground plane and U-shaped slot, thereby achieving wideband performance without the need for additional elements. This method effectively minimizes the surface area of the radiating and ground planes while expanding the bandwidth. While other optimization techniques such as Particle Swarm Optimization (PSO), Differential Evolution (DE), Simulated Annealing (SA), and Ant Colony Optimization (ACO) provide viable alternatives, the Genetic Algorithm (GA) stands out for its efficient global search and fast convergence to optimal solutions, making it the ideal choice for antenna design in this study.

The paper introduces a wideband rectangular MPA designed for satellite applications with a frequency spectrum from 10.26 GHz to 17.28 GHz. The antenna is printed on an FR4 epoxy substrate and has overall dimensions of $18 \times 16 \times 1.6\,\text{mm}^3$ $(0.896\lambda \times 0.797\lambda \times 0.08\lambda)$. Its small size and strong performance characteristics make it well-suited for satellite applications.

This article is divided into six sections. The first section presents the literature review. Section 2 provides a detailed explanation of the genetic algorithm. Section 3 details the antenna structure, including its parameters and the genetic algorithm procedure. Section 4 presents the simulated and measured results and provides a detailed analysis. Section 5 offers a comparative study, and Section 6 summarizes this study.

2. GENETIC ALGORITHM OVERVIEW

Our strategy uses genetic algorithm (GA), as shown in Fig. 1. GA is renowned for its strong and random search abilities, working based on the principles of evolution and natural selection. One of the main strengths of GA is its unique capability to explore solution spaces without imposing restrictions during the optimization process. The effectiveness of the algorithm is highlighted by its adaptive nature, using historical information from previous solution estimates. This innovative approach enables the GA to improve the performance of future solution structures, creating a dynamic and self-improving optimization framework [16]. Consequently, the genetic algorithm is a formidable tool for addressing complex challenges where traditional optimization methods may face limitations [17, 18].

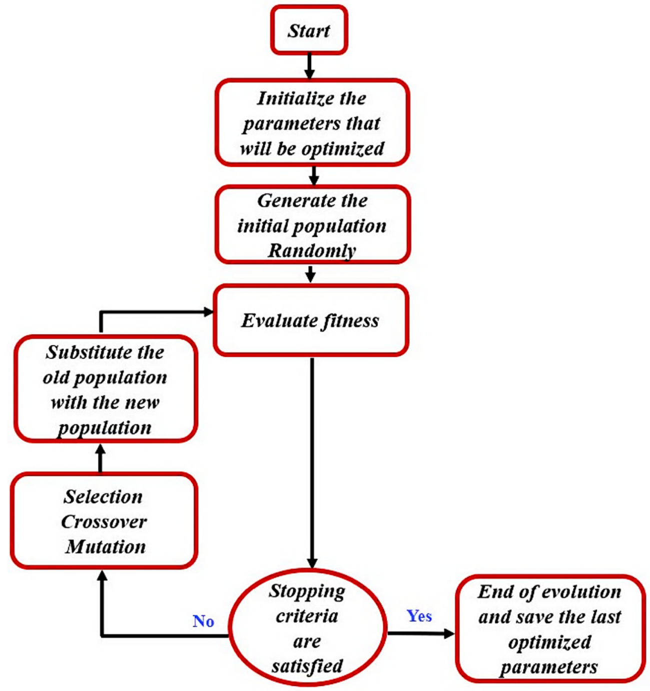

FIGURE 1. Genetic algorithm block diagram.

In genetic algorithm optimization, each individual in the population is typically represented as a sequence of bits. The initial generation is generated randomly to enhance diversity within the population. The effectiveness of each individual is primarily assessed through the cost function, which evaluates their fitness in the specified context.

When these individuals reproduce, a new generation is created. A thorough investigation of the cost function is made possible by the combination of the crossover and mutation processes. The objective is to increase the probability of individuals with higher fitness reproducing, which promotes an iterative process of continuous improvement. This iterative cycle continues through successive steps until a predefined termination condition is satisfied, as detailed in the literature [19, 20]. Fig. 1 encapsulates the fundamental aspects of basic genetic algorithm optimizer with a clear block diagram, demonstrating step-by-step evolution of generations in the quest for optimal solutions.

The key parameters of genetic algorithms that need careful consideration include:

- Crossover Type and Crossover Rate: For an optimization problem, crossover involves exchanging substrings representing chromosomes, which can be a one-point or two-point crossover.

- Mutation: Mutation introduces random changes in the chromosome, altering a gene (bit) to maintain diversity within the population and prevent premature convergence.

- Selection Method: Selection methods identify which individuals within a population will reproduce based on their fitness. Two widely used methods are Roulette Wheel Selection and Tournament Selection. Each method has its own approach to identifying individuals with higher fitness for reproduction.

- Population Size: Population size refers to the number of chromosomes in each generation. A larger population size increases calculation time but improves the solution.
- Number of generations: This parameter specifies the number of iterations for the genetic algorithm (GA) before it meets the stopping criterion. It is crucial in determining the duration and thoroughness of the algorithm's exploration and refinement process.

3. DESIGN METHODOLOGY AND ANTENNA PARAMETERS

A microstrip patch antenna (MPA) is simple, low profile, small, economical, lightweight, and adaptable for both flat and non-flat surfaces. Its fundamental shapes can include a rectangle, a circle, a square, an ellipse, a triangle, a loop, a polygon, or any combination of these shapes to meet specific design requirements [21].

This section describes the design process for the MPA. The process starts by selecting the shape of the antenna and defining its parameters. A rectangle-shaped MPA is chosen to achieve optimal antenna properties. The design is specifically tailored for operation within the Ku-band, covering the spectrum from 10.5 GHz to 14.5 GHz.

The design process starts with an FR4 epoxy substrate with a thickness of 1.6 mm and a dielectric constant of 4.4. This relative permittivity reduces antenna size by lowering the resonant frequency, which is advantageous for compact designs. However, it can also narrow the bandwidth and increase dielectric losses, potentially reducing efficiency. FR4 is favored for its low cost and simple fabrication. Copper, with a thickness (h_t) of 0.035 mm, is used for the ground plane and radiating element.

To connect the microstrip transmission line to the radiating element, an inset feed is utilized to maximize the return loss and ensure the best matching between the microstrip feed line and radiating element. Once we determine these initial design parameters, we will utilize the formulas provided in the cited literature [22, 23] to calculate the remaining physical dimensions of the preliminary antenna.

3.1. The Theoretical Development

This section provides an overview of the mathematical models utilized to estimate the initial dimensions of the rectangular MPA, as mentioned in [18, 23]. Our first step involves calculating the dimensions of the radiating patch.

Our study focuses on an MPA with a rectangular patch characterized by its length (L) and width (W). The patch's width can be estimated by [3, 24]:

$$W = \frac{\vartheta_0}{2f_r}\sqrt{\frac{2}{\varepsilon_r + 1}} \tag{1}$$

where f_r represents the resonant frequency, ϑ_0 the light velocity in free space (3×10^8 m/s), and ε_r the dielectric constant of the substrate. The patch length is defined through the equation below:

$$L = \frac{\vartheta_0}{2f_r\sqrt{\varepsilon_{reff}}} - 2\Delta L \tag{2}$$

Here, L suggests the patch length, and ε_{reff} signifies the effective permittivity, determined by the equation:

$$\varepsilon_{reff} = \frac{\varepsilon_r + 1}{2} + \frac{\varepsilon_r - 1}{2}\left(1 + 12\frac{h}{W}\right)^{-1/2} \tag{3}$$

Substrate thickness is denoted by h. Due to the fringing effect at the edges of the patch, the antenna's electrical dimension exceeds its physical dimension. Consequently, the estimated normalized extension of the patch length ΔL is as follows:

$$\Delta L = 0.412h\frac{(\frac{W}{h} + 0.264)(\varepsilon_{reff} + 0.3)}{(\frac{W}{h} + 0.813)(\varepsilon_{reff} - 0.258)} \tag{4}$$

Using the provided models, the basic antenna design was developed. Table 1 presents the antenna's parametric dimensions, expressed in millimeters.

TABLE 1. Basic antenna parameters.

Design Parameters	Dimensions (in mm)	Details
W_{sub}	18	Substrate width
L_{sub}	16	Substrate length
W_g	18	Ground width
L_g	16	Ground length
W_p	11	Patch width
L_p	7	Patch length
W_f	0.7	Feed line width
L_f	5	Feed line length
H	1.6	Substrate Thickness
h_t	0.035	Ground and patch thickness

3.2. Proposed Antenna Design

In this subsection, we present a new design for rectangular MPA. This design integrates partial ground plane and a centrally placed asymmetric U-shaped slot. The antenna is optimized using genetic algorithm and has an overall dimension of $18 \times 16 \times 1.6\,\text{mm}^3$. The design aims to develop an antenna suitable for the Ku-band frequency range, specifically between 10.5 GHz and 14.5 GHz, while maintaining a compact form factor.

To achieve this, genetic algorithm is used to fine-tune the ground plane length and U-shaped slot dimensions through an iterative optimization process based on the fitness function. The goal is to create an antenna design suitable for satellite applications, departing from the traditional rectangular patch antenna.

The antenna design was simulated using High-Frequency Simulator Software (HFSS), with optimization carried out via genetic algorithm integrated into the HFSS environment through MATLAB. HFSS was chosen for its high precision, robustness, and finite element method (FEM) simulation capabilities, making it ideal for antenna design and genetic algorithm (GA) optimization. The model assumes ideal conditions, excluding factors such as fabrication tolerances, material variations, and environmental influences. Despite these limitations, HFSS effectively predicts antenna performance.

To validate the design, a prototype was constructed, and its performance was compared with simulation and measurement results.

Figure 2 showcases the constructed antenna, which is designed on an FR4 epoxy substrate with a thickness of 1.6 mm, a relative permittivity of 4.4, and a loss factor of 0.02. The structure comprises a rectangular radiating patch featuring a centrally positioned asymmetric U-shaped slot, along with a partially grounded plane.

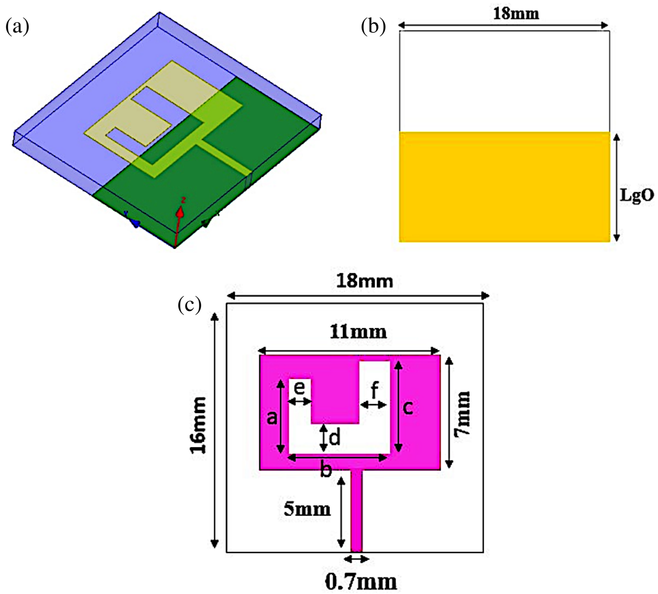

FIGURE 2. Suggested antenna design. (a) Design geometry, (b) front side and (c) back side.

3.3. Antenna Evolution

The design process for the antenna involves three stages, with the antenna size remaining constant throughout. However, the ground plane size evolves as depicted in Fig. 3. In the first stage, mathematical models were used to design a conventional rectangular patch antenna design, having dimensions of $18 \times 16 \times 1.6\,\text{mm}^3$ ($0.416\lambda \times 0.37\lambda \times 0.03\lambda$, where λ is the wavelength at 6.94 GHz), built on an FR4 epoxy substrate chosen for its low cost and ease of fabrication. The radiating patch is rectangular, excited through a microstrip line, and supported by a full ground plane, as illustrated in Fig. 3(a).

In the second stage, depicted in Fig. 3(b), a symmetrical U-shaped slot was introduced at the center of the patch to improve the bandwidth. In the third stage, genetic algorithm is applied to optimize the design by adjusting the slot size and shortening the ground plane. The symmetrical U-shaped slot transforms into an asymmetric U-shaped slot, where one arm of the slot is smaller and the other larger, as illustrated in Fig. 3(c). Additionally, the ground plane is modified from a full to a partial configuration, which further enhances the antenna's performance. This optimization is performed to attain the desired frequency band, as demonstrated in Fig. 4. The combination of the partial ground plane and asymmetric U-shaped slot effectively enhances the antenna's bandwidth.

Figure 4 compares the simulated reflection coefficients for the initial and proposed antennas. The initial antenna resonates around 8.64 GHz, with a reflection coefficient (S_{11}) around -16.37 dB and exhibits a narrow bandwidth, limiting its operational capabilities. In contrast, the proposed antenna significantly improves performance, achieving a wide bandwidth from 10.26 GHz to 17.19 GHz. It exhibits resonance frequencies at 14.94 GHz, as well as an additional resonance at 6.94 GHz. The figure clearly illustrates that adding an asymmetric U-shaped slot and modifying the ground plane effectively improve the antenna's bandwidth.

3.4. Genetic Algorithm Procedure

Our design objective is to attain an S_{11} of at least -10 dB within the frequency bands from 10.5 to 14.5 GHz. To achieve this, we defined the fitness function T, which is maximized during the search to find the most optimal solution, as follows:

$$T = \left| \frac{1}{N} \sum_{i=0}^{N} Q(f_i) \right| \tag{5}$$

with

$$Q(f_i) = \begin{cases} S_{11}(f_i) & \text{for} \quad S_{11}(f_i) \geq -10\,\text{dB} \\ -10\,\text{dB} & \text{for} \quad S_{11}(f_i) < -10\,\text{dB} \end{cases}$$

In the given equation, f_i represents the i-th sampling frequency in the range 10.5–14.5 GHz, N the quantity of samples collected, and S_{11} the coefficient of reflection.

The fitness function T is established to reflect an impedance bandwidth below -10 dB across the specified frequency range. To optimize this function T, as detailed in Equation (5), a new function G is introduced, which needs to be minimized using the genetic algorithm, such as:

$$G = \frac{1}{1+T} \tag{6}$$

The iteration process concludes when the value of G reaches its minimum.

Our optimization approach uses the genetic algorithm to find the optimal parameters for improving antenna performance. There are a total of seven parameters: "L_{go}", "a", "b", "c", "d", "e", and "f", where L_{go} represents the length of the ground plane, while "a", "b", "c", "d", "e", and "f" define the geometric dimensions of the U-shaped slot etched into the patch.

In our design, the optimization procedure consists of several steps illustrated in Fig. 5.

First, an initial population is created randomly. Then, the HFSS software generates and solves a model, with the calculated (S_{11}) parameters automatically retrieved from the main

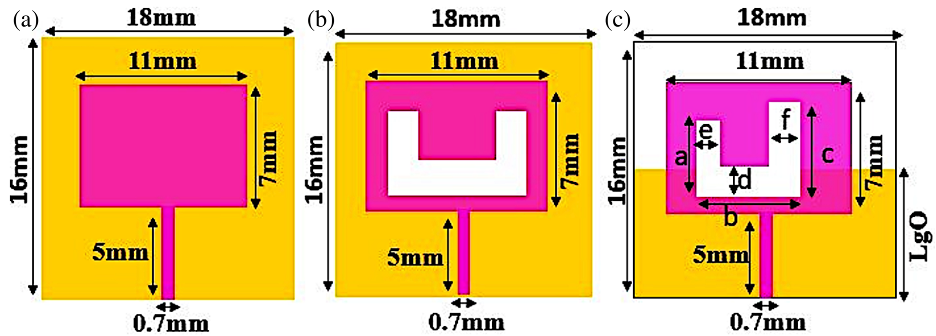

FIGURE 3. Antenna evolution. (a) Stage 1, (b) Stage 2, (c) Stage 3.

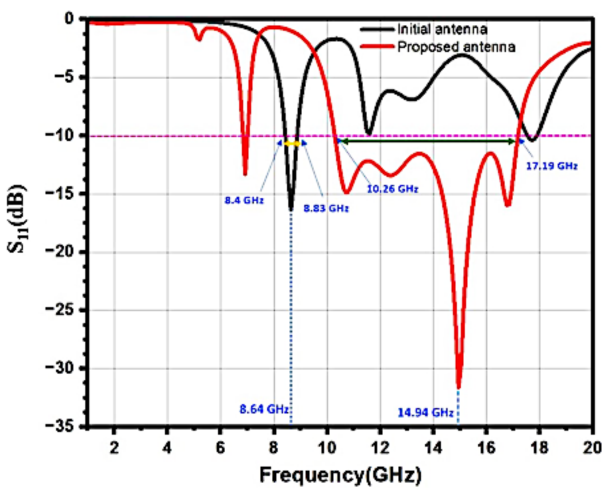

FIGURE 4. Simulated reflection coefficients of both initial and proposed antennas.

Matlab function. The fitness function then evaluates the magnitude of S_{11}. In the next step, genetic algorithm (GA) optimization is applied, and the fitness function is evaluated. If the stopping criterion is met, the process stops; otherwise, it proceeds to the next step. After optimizing the selection of individuals, mutation and crossover are performed. This process continues until the fitness value converges.

The genetic algorithm used to obtain this solution was defined by the following parameters:

- Population size: 30.
- Number of generations: 50.
- Selection: Roulette method.
- Crossover: two points.

Table 2 details the U-shaped slot dimensions and the length of the ground plane, which were optimized using the GA to achieve improved bandwidth performance. With these optimized dimensions, the surface area of the patch was reduced by approximately 71.43%, while the size of the ground plane was minimized by 51.25%.

Figure 6 presents the convergence curve, illustrating the optimization process of the genetic algorithm. The blue line represents the best fitness per generation, while the red dashed

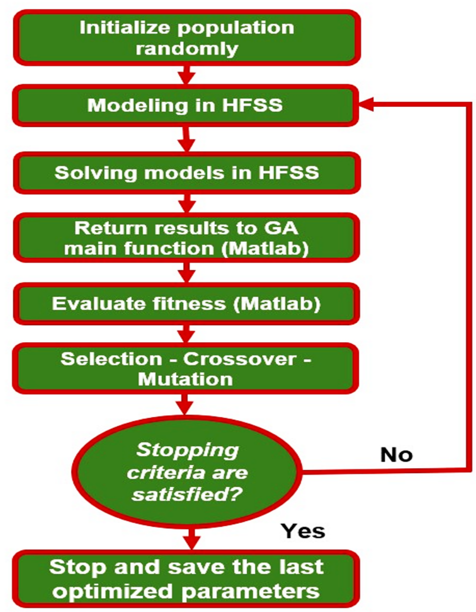

FIGURE 5. Schematic illustration of the adopted Genetic Algorithm.

TABLE 2. Optimized dimensions for the U-shaped slot and the ground plane length.

Design Parameters	Dimensions (in mm)
A	4.63
B	6.43
C	5.68
D	1.62
E	1.23
F	1.94
L_{go}	8.20

line indicates the population's mean fitness. The best fitness improves rapidly in the early generations and stabilizes as the algorithm converges, while the mean fitness follows a similar trend, reflecting the overall improvement of the population. This demonstrates the algorithm's efficiency in exploring the search space and converging to an optimal solution within a reasonable number of generations.

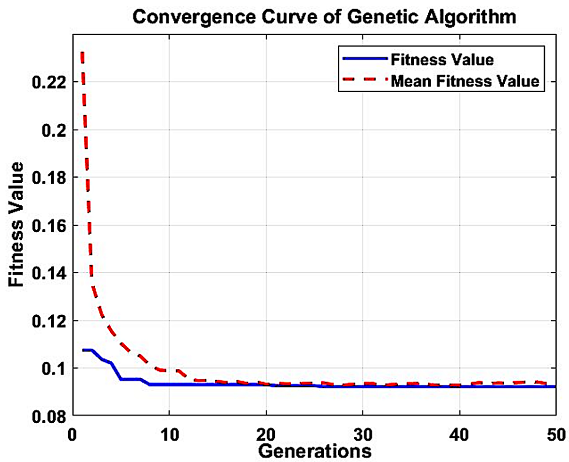

FIGURE 6. Convergence curve of the genetic algorithm.

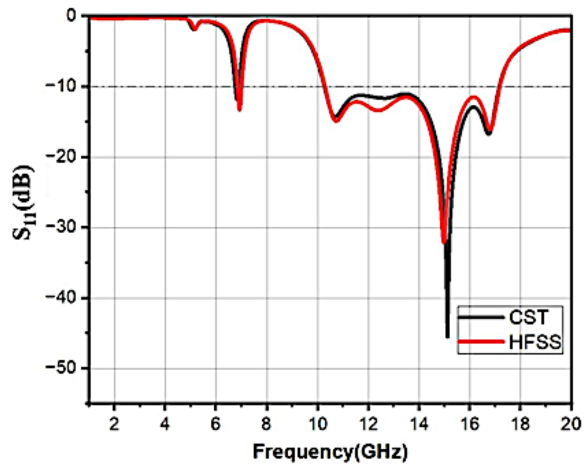

FIGURE 7. Comparison of the simulated S_{11} for the proposed antenna using HFSS and CST.

(a) (b)

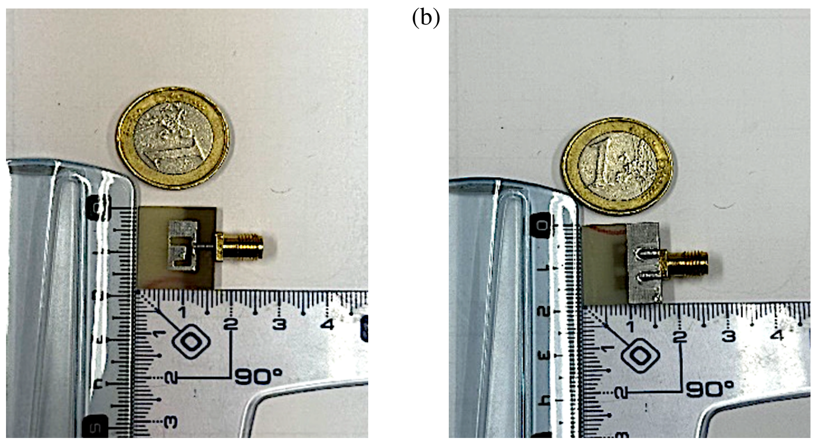

FIGURE 8. Fabricated antenna design: (a) front side and (b) back side.

4. RESULTS AND DISCUSSION

This section concentrates on evaluating the performance of the proposed antenna by analyzing key parameters, including reflection coefficient (S_{11}), voltage standing wave ratio (VSWR), gain, efficiency, and radiation pattern.

4.1. Reflection Coefficient

CST MWS simulators were used to validate the reflection coefficient results from ANSYS HFSS. As shown in Fig. 7, the reflection coefficients from both simulators exhibit consistent variations. The strong agreement between the results confirms the accuracy of the simulations and reinforces the reliability of the proposed design.

As depicted in Fig. 7, the antenna operates across two distinct frequency bands where the reflection coefficient (S_{11}) remains below -10 dB. The first frequency band spans from 6.83 GHz to 7 GHz, with a resonance observed at 6.94 GHz. The second band is a wideband covering 6.93 GHz, from 10.26 GHz to 17.19 GHz, with a resonant frequency of 14.94 GHz. This makes the proposed antenna suitable for direct broadcast services (DBSs) and fixed satellite services (FSSs). Specifically, it can handle FSS frequencies from 14 to 14.5 GHz (transmission) and from 12.2 to 12.7 GHz (reception), as well as DBS frequencies from 11.7 to 12.2 GHz (reception).

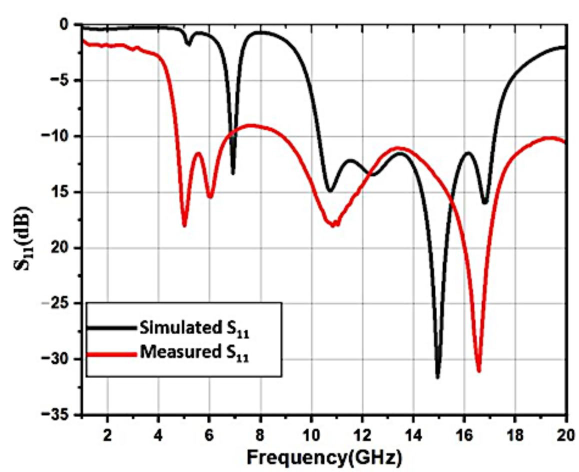

FIGURE 9. Simulated and measured reflection coefficients.

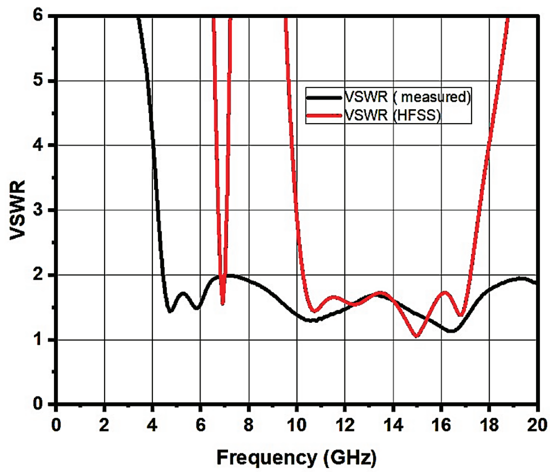

FIGURE 10. The VSWR (Voltage Standing Wave Ratio) for the proposed antenna design.

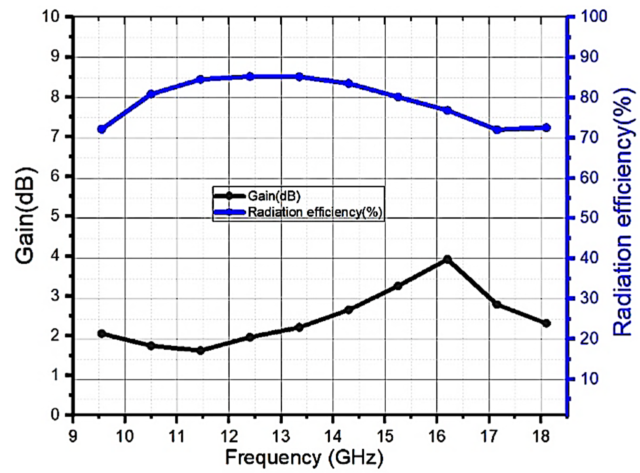

FIGURE 11. Simulated outcomes for the gain and efficiency of the designed antenna.

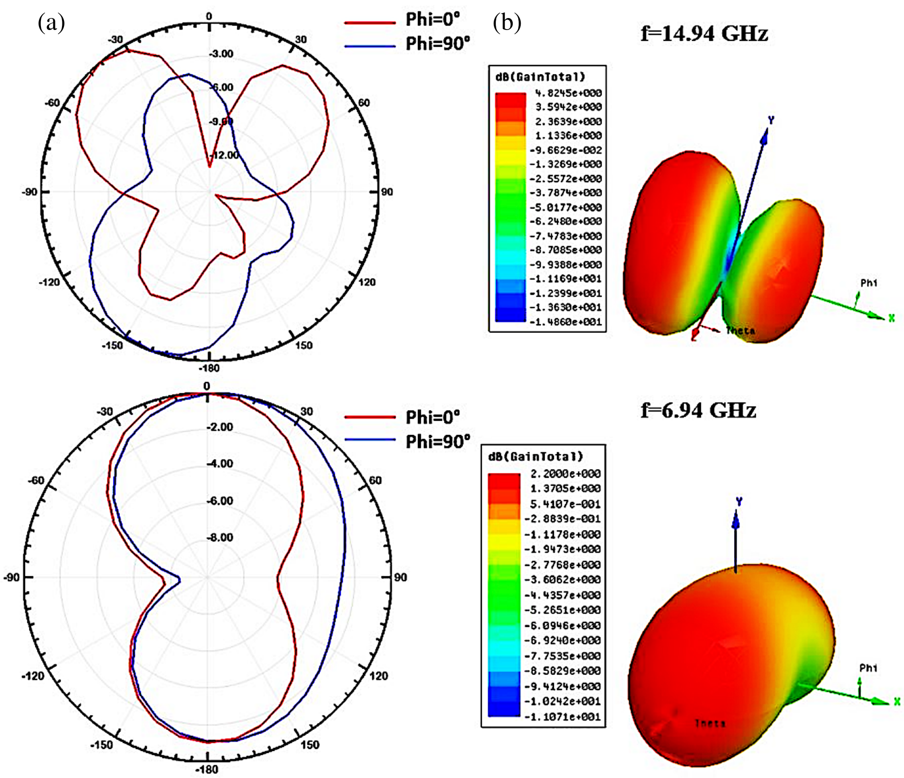

FIGURE 12. Normalized radiation pattern: (a) 2D Illustration and (b) 3D Illustration.

The proposed antenna model was fabricated on an FR4-epoxy substrate, as illustrated in Fig. 8. It was evaluated using a Vector Network Analyzer 3656D, with a frequency range from 300 KHz to 20 GHz. The effectiveness of the proposed antenna was validated by comparing the prototype's performance with the simulation results.

Figure 9 shows that the measured S_{11} for the prototyped antenna exhibits two distinct bands: the first covers 1.93 GHz, ranging from 4.71 GHz to 6.64 GHz, and the second is a wide band spanning 10.41 GHz, from 8.92 GHz to 19.33 GHz. These measured results align with the simulated ones, demonstrating strong agreement. Although minor differences exist between the measured and simulated results, they can be attributed to fabrication imperfections, material property variations, and measurement uncertainties.

4.2. Voltage Standing Wave Ratio (VSWR)

The VSWR should ideally be less than 2 for the operating bandwidth [3]. Fig. 10 illustrates both the simulated and measured VSWRs of the proposed antenna. As seen, the simulated VSWR is less than 2 across the satellite band (from 10.26 GHz

TABLE 3. Comprehensive and detailed comparison of the antenna design's performance against previous research.

Ref.	Year	Antenna size (mm^3)	Substrate material	Operating band (GHz)	Band width (GHz)	Resonant frequency (GHz)	Applications
[25]	2020	$20 \times 20 \times 1.6$	FR-4	11.4–12.98 14.21–14.86 17.41–18.98	1.58 0.65 1.57	12.25 14.16 17.50	Ku-Band
[11]	2021	$40 \times 48 \times 1.59$	FR-4	12.8–15.83	3.03	14	Ku-Band
[26]	2021	$30 \times 30 \times 1.6$	FR-4	13.6–18.56	4.96	14.5	Ku-Band
[12]	2021	$40 \times 40 \times 1.6$	FR-4	11.595–15.75	4.1553	12.54	Ku-Band
[27]	2022	$20 \times 20 \times 1.6$	FR-4	11.0–11.5 11.8–12.3 13.0–14.3	0.5 0.5 1.3	11.36 12.14 13.4	X and Ku-band
[28]	2023	$34 \times 35 \times 1.6$	FR-4	13.6–18.56	2.4	14	Ku-Band
[14]	2023	$27 \times 26 \times 1.6$	FR-4	12.2–13.5 14.8–16.4	1.3 1.6	12.7 15.6	Ku-Band
[29]	2023	$20 \times 20 \times 1.6$	FR-4	12.5–14.9 16.0–19.3	2.4 3.3	12.9 17.1	Ku-Band
[4]	2024	$40 \times 40 \times 0.508$	Rodgers RT5880	15.16–17.16	2	16	Ku-Band
[30]	2024	$25 \times 25 \times 1.635$	FR-4	16.31–17.18	0.867	16.694	Ku-Band
[15]	2024	$20 \times 20 \times 1.6$	FR-4	11.25–13.6	2.35	12.62	Ku-band
Proposed	2025	$18 \times 16 \times 1.6$	FR-4	6.83–7 10.26–17.19	0.17 6.91	6.94 14.94	X and Ku-Band

to 17.19 GHz), reflecting the high efficiency of the simulated microstrip patch antenna. This simulated result is in good agreement with the measured ones, confirming the antenna's effective performance.

4.3. Gain and Efficiency

Figure 11 displays the simulated gain and radiation efficiency of the antenna. We remark that the gain rises across the operational frequency range from 10.26 GHz to 17.19 GHz, achieving a maximum value of 4 dB. This result indicates that the proposed antenna design provides good gain across its operational band. Additionally, the radiation efficiency is between 75% and 84%, reflecting effective radiation across the entire frequency range.

4.4. Radiation Pattern

The 2D normalized radiation patterns for the far-field region were evaluated in two principal cut-planes: XZ-plane ($\phi = 0°$) and YZ-plane ($\phi = 90°$), corresponding to H-plane and E-plane, respectively. These patterns were analyzed at its two primary resonance frequencies of 14.94 GHz and 6.94 GHz as illustrated in Fig. 12(a). The corresponding 3D radiation pattern is presented in Fig. 12(b). The proposed antenna demonstrates a bidirectional radiation pattern with a peak gain of 4.82 dB at 14.94 GHz, whereas at 6.94 GHz, it exhibits an omnidirectional radiation pattern with a peak gain of 2.2 dB.

5. COMPARATIVE STUDY

Table 3 presents a performance comparison between the proposed antenna design and various Ku-band antennas proposed in the literature. Compared to other published designs, the proposed antenna offers notable advantages, including a wide bandwidth (from 10.26 GHz to 17.19 GHz), compact size, good radiation level, and good gain. The proposed work introduces a novel approach to enhancing the bandwidth of microstrip patch antenna without increasing its volume. These exceptional characteristics make the antenna particularly suitable for Ku-band satellite applications.

6. CONCLUSION

This article introduces the design of a compact, high-efficiency wideband microstrip patch antenna optimized for satellite applications. The proposed antenna incorporates an asymmetric U-shaped slot and a partial ground plane, with a genetic algorithm used to fine-tune their dimensions and enhance bandwidth while maintaining a compact form factor. With dimensions of $18 \times 16 \times 1.6\,mm^3$ and being fabricated on an FR-4 epoxy substrate, the antenna offers a cost-effective and manufacturable solution for modern satellite systems. The measured results indicate that the optimization successfully expands the bandwidth of the proposed antenna without increasing the antenna's physical volume, achieving dual-band operation from 4.71 GHz to 6.64 GHz (1.93 GHz bandwidth) and 8.92 GHz to

19.33 GHz (10.41 GHz bandwidth), with a maximum gain of 4 dB. These results highlight the antenna's effectiveness and suitability for fixed satellite services (FSSs) and direct broadcast services (DBSs), demonstrating an optimal balance between size, bandwidth, and efficiency. The successful application of genetic algorithm-based optimization underscores its potential for enhancing antenna performance without increasing design complexity. Future research could explore advanced low-loss substrates, alternative feeding techniques, and multi-objective optimization to further improve gain, polarization purity, and radiation efficiency.

ACKNOWLEDGEMENT

The authors would like to thank Universiti Teknikal Malaysia Melaka (UTeM) and the Ministry of Higher Education (MOHE) of Malaysia for supporting this project.

REFERENCES

[1] Maral, G., M. Bousquet, and Z. Sun, *Satellite Communications Systems: Systems, Techniques and Technology*, John Wiley & Sons, 2020.

[2] Elabd, R. H. and A. J. A. Al-Gburi, "Design and optimization of a circular ring-shaped UWB fractal antenna for wireless multi-band applications using particle swarm optimization," *Progress In Electromagnetics Research B*, Vol. 106, 101–112, 2024.

[3] Kumar, P., A. K. Singh, R. Kumar, S. K. Mahto, P. Pal, R. Sinha, A. Choubey, and A. J. A. Al-Gburi, "Design and analysis of low profile stepped feedline with dual circular patch MIMO antenna and stub loaded partial ground plane for wireless applications," *Progress In Electromagnetics Research C*, Vol. 140, 135–144, 2024.

[4] Chrij, D., A. Khabba, Z. E. Ouadi, L. Sellak, J. Amadid, O. Benkhadda, S. Ibnyaich, A. Zeroual, and A. J. A. Al-Gburi, "A low-cost wideband SIW antenna with bilateral slots on FR4 epoxy for ku-band applications," *Progress In Electromagnetics Research M*, Vol. 131, 61–70, 2025.

[5] Zerrad, F.-E., M. Taouzari, E. M. Makroum, J. E. Aoufi, S. D. Qanadli, M. Karaaslan, A. J. A. Al-Gburi, and Z. Zakaria, "Microwave imaging approach for breast cancer detection using a tapered slot antenna loaded with parasitic components," *Materials*, Vol. 16, No. 4, 1496, 2023.

[6] Al-Gburi, A. J. A., M. M. Ismail, N. J. Mohammed, and T. A. H. Alghamdi, "SAR flexible antenna advancements: Highly conductive polymer-graphene oxide-silver nanocomposites," *Progress In Electromagnetics Research M*, Vol. 127, 23–30, 2024.

[7] Jetti, C. R., T. Addepalli, S. R. Devireddy, G. K. Tanimki, A. J. A. Al-Gburi, Z. Zakaria, and P. Sunitha, "Design and analysis of modified U-shaped four element MIMO antenna for dual-band 5G millimeter wave applications," *Micromachines*, Vol. 14, No. 8, 1545, 2023.

[8] Gupta, A., V. Kumar, D. K. Garg, and A. J. A. Al-Gburi, "Machine learning-based reflection coefficient and impedance prediction for a meandered slot patch antenna," *Materials Science in Semiconductor Processing*, Vol. 188, 109245, 2025.

[9] Al-Gburi, A. J. A., I. Ibrahim, Z. Zakaria, and A. D. Khaleel, "Bandwidth and gain enhancement of ultra-wideband monopole antenna using MEBG structure," *ARPN Journal of Engineering and Applied Sciences (JEAS)*, Vol. 14, 3390–3393, 2019.

[10] Kumar, P., A. K. Singh, R. Kumar, S. K. Mahto, P. Pal, R. Sinha, A. Choubey, and A. J. A. Al-Gburi, "Design and analysis of low profile stepped feedline with dual circular patch MIMO antenna and stub loaded partial ground plane for wireless applications," *Progress In Electromagnetics Research C*, Vol. 140, 135–144, 2024.

[11] Davuluri, A. J. and P. Siddaiah, "Design of wide band slotted microstrip patch antenna with defective ground structure for Ku band," *International Journal of Electrical and Computer Engineering*, Vol. 11, No. 2, 1337, 2021.

[12] Islam, M. T., M. S. Mahmud, M. H. Islam, A. Shahriar, S. S. Islam, M. R. I. Faruque, and A. H. Gulib, "Design of a microstrip patch antenna for the Ku band applications," *Materials Today: Proceedings*, Vol. 42, 1502–1505, 2021.

[13] Kourav, S., K. Verma, J. K. Ahirwar, S. K. Shah, M. Jangid, and Y. S. Thakur, "The design and analysis of a high bandwidth patch antenna loaded with double-L shaped parasitic and super-strate components," *Journal of Telecommunication, Switching Systems and Networks*, Vol. 10, No. 2, 1–13, 2023.

[14] Behera, H. K. and L. P. Mishra, "Circularly polarized cup shaped patch antenna for Ku band application," *Journal of Statistics & Management Systems*, Vol. 26, No. 1, 35–41, 2023.

[15] Malisuwan, S., J. Sivaraks, N. Madan, and N. Suriyakrai, "Design of microstrip patch antenna for Ku-band satellite communication applications," *International Journal of Computer and Communication Engineering*, Vol. 3, No. 6, 413, 2014.

[16] Lamsalli, M., A. E. Hamichi, M. Boussouis, N. A. Touhami, and T. Elhamadi, "Genetic algorithm optimization for microstrip patch antenna miniaturization," *Progress In Electromagnetics Research Letters*, Vol. 60, 113–120, 2016.

[17] Wakrim, L., A. E. Yassini, A. Khabba, S. Ibnyaich, and M. M. Hassani, "Novel design of a triple band PIFA antenna by using a binary genetic algorithm," *Journal of Computational Electronics*, Vol. 20, 1373–1386, 2021.

[18] Bennioui, F.-Z., A. Khabba, K. A. Bouslam, L. Wakrim, S. Ibnyaich, and A. Zeroual, "Genetic algorithm-based optimization of rectangular patch antenna parameters for 2.45 GHz," in *2024 International Conference on Global Aeronautical Engineering and Satellite Technology (GAST)*, 1–6, Marrakesh, Morocco, 2024.

[19] Johnson, J. M. and Y. Rahmat-Samii, "Genetic algorithms and method of moments (GA/MOM) for the design of integrated antennas," *IEEE Transactions on Antennas and Propagation*, Vol. 47, No. 10, 1606–1614, 1999.

[20] Jayasinghe, J. W., "Application of genetic algorithm for binary optimization of microstrip antennas: A review," *AIMS Electronics and Electrical Engineering*, Vol. 5, No. 4, 315–333, 2021.

[21] Balanis, C. A., *Advanced Engineering Electromagnetics*, John Wiley & Sons, 2012.

[22] Garg, R., *Microstrip Antenna Design Handbook*, Artech House, 2001.

[23] Hammerstad, E. O., "Equations for microstrip circuit design," in *1975 5th European Microwave Conference*, 268–272, Hamburg, Germany, 1975.

[24] Jain, P., P. K. Sahoo, A. D. Khaleel, and A. J. A. Al-Gburi, "Enhanced prediction of metamaterial antenna parameters using advanced machine learning regression models," *Progress In Electromagnetics Research C*, Vol. 146, 1–12, 2024.

[25] Al-Gburi, A. J. A., I. M. Ibrahim, and Z. Zakaria, "An ultra-miniaturized MCPM antenna for ultra-wideband applications," *Journal of Nano- and Electronic Physics*, Vol. 13, No. 5, 2021.

[26] Satrusallya, S. and M. N. Mohanty, "Design of antenna array for Ku-band wireless application," *Instrumentation Mesure*

Métrologie, Vol. 20, No. 2, 107–112, 2021.

[27] Singh, S., K. Srivastava, F. Usman, and R. S. Yadav, "Bat shaped circularly polarized antenna for X and Ku band applications," *Progress In Electromagnetics Research C*, Vol. 119, 235–244, 2022.

[28] Keshwala, U., S. Rawat, and K. Ray, "Circularly polarized truncated corner square slot antenna for Ku-band applications," *Scientia Iranica*, Vol. 30, No. 1, 218–227, 2023.

[29] Patil, K. N., M. T. Raj, K. A. Chethana, A. K. Dwivedi, N. K. Narayanaswamy, and V. Singh, "Compact ultra-wideband multilayer patch antenna with defected ground plane for Ku band applications," *Microwave Review*, Vol. 29, No. 1, 2023.

[30] Kumar, S. A. and R. M. Chadhar, "Design and performance of square microstrip patch antenna for super wide band," *International Journal of Scientific Research & Engineering Trends*, Vol. 10, No. 2, 458–462, 2024.